Contents lists available at ScienceDirect

Talanta

journal homepage: http://ees.elsevier.com

A modified mid-level data fusion approach on electronic nose and FT-NIR data for evaluating the effect of different storage conditions on rice germ shelf life

Cristina Malegori [a,*], Susanna Buratti [b], Simona Benedetti [b], Paolo Oliveri [a], Simona Ratti [b], Carola Cappa [b], Mara Lucisano [b]

[a] DIFAR Department of Pharmacy, University of Genova, Genova, Italy
[b] DeFENS Department of Food, Environmental and Nutritional Sciences, Università degli Studi di Milano – Milano, Italy

ARTICLE INFO

Keywords
E-nose
MOS sensor
FT-NIR
Correlation map
Data fusion
Rice germ

ABSTRACT

Evaluating the possibility of extending shelf life of rice germ (a by-product of rice milling process) by reducing water activity in combination with storage atmosphere packaging, without any heat treatment, is the aim of the present study. Samples at different water activities (0.55, 0.45 and 0.36) were packed in air, argon or under vacuum, and stored at 27 °C for 150 days. To the aim, a non-targeted approach was applied by means of an FT-NIR spectrometer in reflectance with a rotating sample holder and a portable electronic nose, equipped with 10 non-specific sensors. For understanding the impact of the factors under study on the rice germ shelf life, a modified mid-level data fusion approach was applied to enhance the information most correlated with time. Moreover, Principal Component Analysis was applied on fused data to follow samples evolution during storage and identify different clusters according to the storage conditions. The rice germ case study allowed to better understand the information captured by the non-specific sensors: a 2D correlation map was developed combining the e-nose data with the NIR spectral information, highlighting relationships among NIR absorption bands and classes of chemical compounds inducing e-nose responses. A data fusion approach highlighted the importance of water activity on rice germ storage, while no interesting differences were ascribable to storage atmosphere packaging systems. In terms of correlation, the sensors could be divided in two groups, negatively inter-correlated: sensors ascribable to aromatic compounds (WC) and correlated with the NIR band around 4800–4900 cm^{-1} (N–H bending of primary amides, typical for peptides coming from protein hydrolysis); broad-range response sensors (WS), linked with the NIR band at 5128 cm^{-1} (second overtone of C═O stretching of esters).

1. Introduction

During brown rice milling, a by-product containing bran layers and germ is obtained. This by-product, usually intended for animal feed, contains about 16–20% of rice germ, an interesting material for human consumption as a source of proteins, fibres, minerals, vitamins, lipids rich in unsaturated fatty acids and bioactive phytochemicals, like γ-orizanol, tocopherols, and tocotrienol useful for their health-promoting properties and antioxidant activity [1]. Rice germ may have a broad range of application, such as in baked products, snack foods, breakfast cereals, or for oil extraction for food and cosmetic industries. However, the high fat content of germ, ranging from 20 to 25%, and the presence of unsaturated fatty acids and lipolytic enzymes promote the onset of hydrolytic and oxidation phenomena causing the development of off-flavours, responsible for the germ quality decay and the reduced shelf life. Stabilisation processes have been widely applied to rice bran just after milling. Literature refers that, in most of the cases, heat is applied through different technological procedures: dry heating or extrusion [2], steaming [3], infrared radiation [4], microwave [5] or ohmic heating [6]. Other techniques proposed to slow down oxidations include refrigeration, acidification or storage at low temperatures [7]. A potential solution to extend the shelf life of rice germ or bran is the use of storage atmospheres, coupled with packaging materials that can exert a barrier effect against light, moisture and oxygen [8]. To study the quality decay of food having high fat content, such as rice germ, many techniques have been applied.

The electronic nose (e-nose) to some extent mimics the human sense of smell and, in this work, it has been applied for the first time as simple, fast and non-destructive method to follow the evolution of rice germ volatile profile during storage. E-nose technology is based on an array of sensors for gases, whose outputs are integrated by advanced signal processing to rapidly evaluate the odour fingerprint of the analysed products [9,10]. According to previous works, e-nose is suitable for the discrimination of olive oil [11] and of different stages

* Corresponding author. Viale Cembrano, 4 – 16148, Genova (GE), Italy.
E-mail address: malegori@difar.unige.it (C. Malegori)

https://doi.org/10.1016/j.talanta.2019.120208
Received 17 May 2019; Received in revised form 23 July 2019; Accepted 31 July 2019
Available online xxx
0039-9140/

of lipid oxidation on vegetable oils [12–14]. On rice samples, e-nose has been applied for odour classification [15], for quality assessment during storage at different temperatures [16] and for discriminating different damages of rice plants [17].

Vibrational spectroscopy in the near infrared (NIR) region (12,000-4000 cm^{-1}) is a non-destructive analytical method, widely applied for qualitative and quantitative determinations of chemicals in several fields, including environmental [18], pharmaceutical [19,20] and food applications [21]. Moreover, Fourier-transform NIR (FT-NIR) spectroscopy has been applied for characterising rice in terms of chemical composition [22], authentication [23] and automatic inspection [24]. No evidences about the application of such a spectroscopy for the study of rice germ shelf life are encountered in the literature; until now, FT-NIR has been applied on rice bran oil samples only for the quantitative determination of γ-oryzanol [25].

This study explores the possibility of extending the shelf life of rice germ by reducing water activity in combination with storage atmosphere packaging, without any heat treatment. In order to assess the quality of this by-product during storage, a non-targeted approach was applied by combining a portable e-nose and an FT-NIR spectrometer. To this aim, the information embodied in e-nose signals and FT-NIR spectra was joint by a modified mid-level data fusion approach. Data fusion is a robust method for creating multi-block data sets [26], already applied for merging FT-NIR data and e-nose responses [27,28]. In the present study, for the first time, variable compression, needed for a mid-level fusion, is performed taking into account the time trend; in this way, sample evolution was strongly highlighted in both of the subsets of data before combination.

The study of the correlation between the two subsets of data is another innovative task of this work, which allows to understand the chemical information carried by the e-nose sensors. The building of a Pearson's correlation map between FT-NIR spectra and MOS sensor responses highlights strength and direction of correlation between the most important absorption NIR bands and the sensors considered as crucial for explaining rice germ shelf life [29]. This step of data processing, in fact, allows to understand the relation between different non-selective analytical techniques, in terms of characterisation of a specific set of samples. In this way, a joint interpretation of the whole information is made possible, permitting a straightforward comprehension of a phenomenon/process from a chemical point of view. This approach is especially powerful when the analytical techniques considered are complementary and just one of them is not enough for a complete characterisation. Thanks to the chemometric protocol proposed, a chemical understanding of rice germ modification during storage is outlined.

2. Materials and method

2.1. Experimental plan

Rice germ was provided by Società Agricola Cooperativa Rondolino (Livorno Ferraris, Vercelli) and separated from the bran through sifting to a purity degree of 86%.

In order to understand the influence of water activity (a_w) and storage atmosphere (SAP) on rice germ shelf life, the two factors were set at three different levels, as reported in Fig. 1. To reduce moisture, rice germ was dried in a vacuum oven (WIPA, etc.) at 40 °C, from the original moisture value of 9.71 ± 0.11 g/100 g (coded with A) to 7.82 ± 0.15 g/100 g (coded with B), and 6.86 ± 0.08 g/100 g (coded with C). Germ moisture was determined gravimetrically, as the average of two determinations, after drying at 105 °C until constant weight. According to germ moistures, different water activities were obtained: 0.55 (corresponding to moisture codified with A), 0.45 (corresponding to moisture codified with B), and 0.36 (corresponding to moisture codified with C). Water activity values were determined by using an Aqualab 3TE (Decagon Devices Inc., USA) previously calibrated with a standard solution (a_w = 0.50).

Germ with the highest moisture content (A) was packed only in air (coded with 1) as it represents the low-cost commonly used strategy to store rice germ, while samples B and C were packed also under vacuum (coded with 2) and in argon (coded with 3). All samples (130 g each) were packed in 210 mL aluminium cans. A total of 70 cans were prepared and stored at 27 °C ± 1 for 150 days and 5 sampling times were studied (T1, T2, T3, T4, T5 after 30, 60, 90, 120, and 150 days of storage, respectively). Samples were identified with one letter (A, B, C)

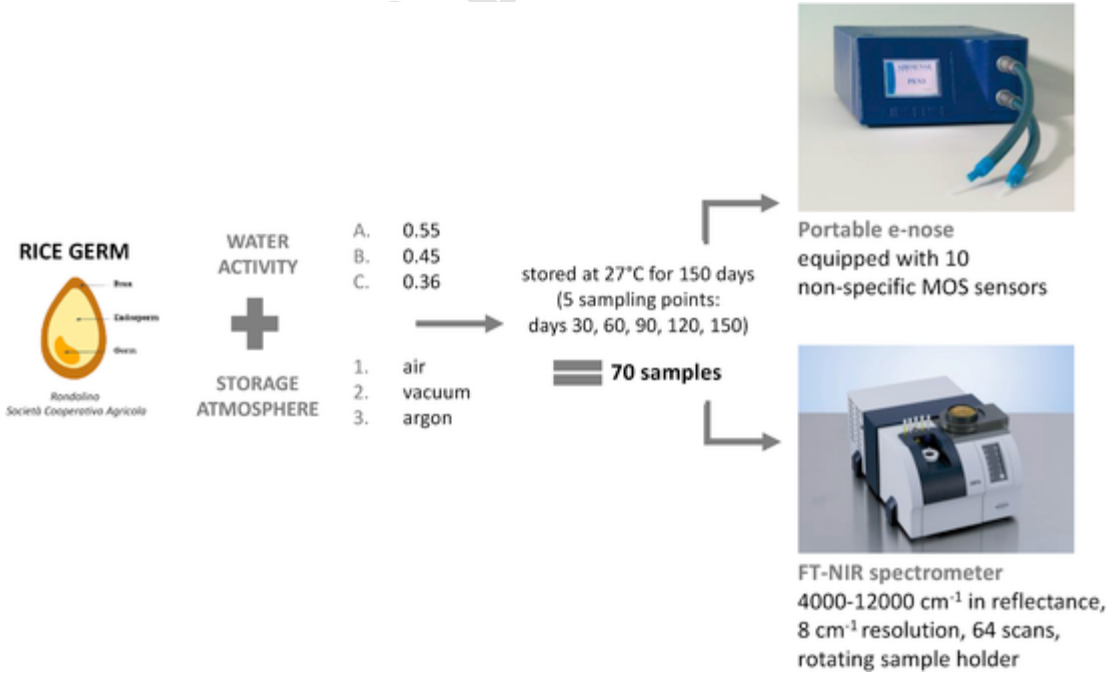

Fig. 1. Graphical representation of the experimental plan.

related to aw and one number (1, 2, 3) according to the type of modified atmosphere packaging; two cans were analysed for each combination of a_w level and SAP type, for a total of 14 samples at each sampling time (samples A1, B1, B2, B3, C1, C2, C3 in replicates). It is important to point out that rice germ at the three different a_w was analysed also before packaging for a total of 6 samples, two technological replicates (cans) for each a_w condition.

The detailed sampling plan is detailed in Table 1.

2.2. E-nose analysis

Volatile profile of rice germ samples was determined by a Portable Electronic Nose (PEN2, Win Muster Airsense Analytics Inc., Schwerin, Germany). The device consists of a sampling apparatus, a detecting unit with a sensor array, and an appropriate software (Win Muster v.1.6) for data recording. The sensor array is composed by 10 metal oxide semiconductor (MOS) type sensors [28]: W1C (aromatic); W5S (broad-range); W3C (aromatics); W6S (hydrogen); W5C (aromatics–aliphatics); W1S (broad-methane); W1W (sulphur-containing compounds); W2S (broad-alcohol); W2W (sulphur-containing and chlorinated compounds); W3S (methane-aliphatics).

For the determination of the aromatic profiles of rice germ, 3 g of sample were placed in a 30 mL airtight glass vial fitted with a pierceable silicon/Teflon® septum. After 4-h equilibration at room temperature, headspace measurements were performed according to the following conditions: flow rate 300 mL/min, injection time 60 s, flush time 180 s (during which the surface of the sensors was cleaned with air filtered through active carbon). All samples were analysed in duplicate and the averages of sensor responses were used for subsequent statistical analysis.

Table 1
Sampling plan.

TIME	TOTAL DAYS OF STORAGE	N. OF SAMPLES	SAMPLE IDENTIFICATION	CANS
T1	30	14	A1, B1, B2, B3, C1, C2, C3	2
T2	60	14	A1, B1, B2, B3, C1, C2, C3	2
T3	90	14	A1, B1, B2, B3, C1, C2, C3	2
T4	120	14	A1, B1, B2, B3, C1, C2, C3	2
T5	150	14	A1, B1, B2, B3, C1, C2, C3	2

Germ water activity: A = 0.55; B = 0.45; C = 0.36.
Packaging atmosphere: 1 = air; 2 = under vacuum; 3 = argon.

2.3. FT-NIR acquisition

For acquiring the spectroscopic data, a Fourier Transform NIR spectrometer (MPA device – Bruker Optics, Milan, Italy) equipped with a rotating sample holder was used; spectra were acquired in the range 12,000–4000 cm^{-1}, with a 8 cm^{-1} resolution, and 64 scans for both samples and background. For obtaining a representative spectrum of each sample, the whole content of rice germ coming from each can was placed in a glass Petri dish at room temperature (20–22 °C) before performing the rotational acquisition.

2.4. Data processing

2.4.1. Data fusion

Focusing on FT-NIR data, the pseudo-absorbance spectra were pre-processed by means of the standard normal variate (SNV) transform [30] to reduce the effect of total intensity, as presented in Fig. 2a; in this work, a tailor made data centering (called t0 centering) is proposed to minimise differences among batches, enhancing the information related with the time trend (Fig. 2b). The t0 centering is performed subtracting the mean spectrum at t0 from the FT-NIR profiles along time, at the same a_w; to better clarify this approach, for example, from all the B samples (at different SAP and time), the mean spectrum of two B1 cans at t0 was subtracted. The same approach was followed also on e-nose data. In this way, after pre-processing, samples of t0 coming from the two blocks of data were mathematically set at zero, in the same way as the global mean for a traditional mean centering. To the aim of understanding the rice germ shelf life, with t0 centering, the changes along time were highlighted while differences among storage conditions were reduced.

In this study, a non-targeted approach based on the combination between e-nose and FT-NIR was applied. In fact, the e-nose device is devoted to the evaluation of volatile fraction while the NIR spectrometer allows to understand chemical composition of the samples under study; the combination of these different sources of information gives a comprehensive understanding of rice germ characteristic evolution.

To properly combine the two blocks of data, a modified mid-level data fusion was proposed; this approach, firstly, extracts some relevant features from each block separately and, then, concatenates the features into a single array, suitable for further multivariate data processing [26]. According to this procedure, the FT-NIR spectra were modelled by Partial Least Squares (PLS) regression using, as the response variable, a vector containing the sampling time. Thanks to this supervised approach, new variables (called latent variables – LVs) are computed as the direction of maximum covariance between FT-NIR data and time, strongly emphasising chemical modifications that occurred during rice germ storage. For these reasons, the regression approach was more appropriate, as a data compression step, than an exploratory method such as PCA. Regarding the e-nose responses, a modification of the mid-level procedure is proposed for the first time. In fact, for e-

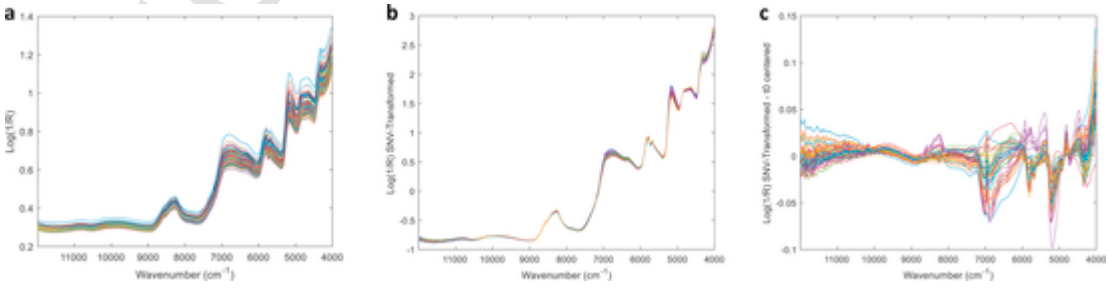

Fig. 2. NIR spectra: a) raw signals, b) SNV-transformed signals, c) t0 centered data.

nose block, the data reduction was performed not by compression algorithms (like PLS for FT-NIR data) but by means of data selection: the sensors submitted to data fusion were the ones most strongly correlated with time. Strength and direction of the correlation were calculated as Pearson's correlation coefficient, ranging from −1 (negatively strongly correlated) and 1 (positively strongly correlated), where 0 represents the absence of correlation [29]. In Fig. 3, a scheme of the modified mid-level data fusion proposed in this work is outlined, to better explain the contribution of each data block in understanding the rice germ shelf life. On the two blocks of data, properly fused, a final PCA was applied as an unsupervised exploratory approach; the joint evaluation of score and loading plots allowed to observe trends and groupings within samples and to understand relationships between the two blocks of variables.

The whole data processing was performed under the Matlab® environment (The MathWorks, Inc., Natick, MA, USA, Version 2017a), thanks to the implementation of customised algorithms.

2.4.2. Correlation matrix

A key task in the present study was the ascription of a chemical meaning to the MOS non-specific sensors; to the aim, a correlation map between sensors and NIR variables was built. The map is a graphical representation of Pearson's correlation coefficient calculated between couples of variables. This coefficient expresses the type of sample distribution in the bivariate space defined by each couple of variables; as presented in paragraph 2.4.1, it can vary between −1 and 1. This procedure was applied for understanding both the correlation between sensors and FT-NIR spectra, and the correlation between one sensors and all the others. In this way, patterns/families of sensors were identified, evaluating if correlated sensors were also united by the same chemical information. This approach was already used in a previous research work for studying correlation between fingerprint signals, such as near- and mid-infrared spectra [31], but no evidences were found in the literature for correlation maps between spectral data and e-nose responses.

3. Results and discussion

In the following paragraph, results are presented separately in two sections focusing, one by one, on the two main aims of the study. The first section deals with rice germ shelf life, intended as the evaluation of storage factors (a_w and SAP) on sample degradation; the second one is aimed at attributing a chemical meaning to the non-specific MOS sensors, thanks to the correlation with FT-NIR data. The understanding of such analytical evidences allows a comprehensive discussion about rice germ chemical modifications along time, together with an in-depth understanding of the non-targeted approach applied.

3.1. Rice germ shelf life

For understanding the influence of a_w and SAP on rice germ shelf life, a preliminary PCA on fused data was performed. The data array that was submitted to exploratory analysis was built combining the 4 MOS sensors most related with time and the 4 lowest-order latent variables of the PLS model (computed with FT-NIR data as the predictors and the time vector as the response). The Pearson's correlation coefficients between time and the 10 non-specific sensors of the e-nose are the following: W1C = −0.76; W5S = 0.15; W3C = −0.76; W6S = 0.05; W5C = −0.69; W1S = 0.30; W1W = 0.24; W2S = 0.53; W2W = 0.10; W3S = 0.09. Only the 4 sensors with a correlation coefficient higher than 0.5, as absolute value, were selected as interesting for describing rice germ shelf life; the selected sensors are: W1C, W3C, W5C and W2S. According to the number of variables chosen for the e-nose data block, also for the FT-NIR block, only 4 latent variables were retained; in this way, the two data blocks had the same weight in the multi-block array, now suitable for further data processing. Moreover, the error in cross-validation (5 deletion groups) was almost the same (around 5 days) for model complexity lower then 5LVs and showed a noticeable increase for higher LV numbers, as reported in Fig. 3.

In Fig. 4, results of PCA on fused data are presented. In more detail, score plots and loading plots of PC1 *vs.* PC3 are presented allowing to identify sample patterns and variable imputation, respectively. The score plot (Fig. 4a), explaining 71.7% of the whole variance of the multi-block array, shows a trend of the rice germ samples according to the storage time. This trend is clearer along PC1 and, in particular, samples at the beginning of the storage are located at positive values of the component, moving at negative values with the progress of time. The fact that PC1, explaining the highest amount of variance (57.3%), is imputable to the time trend was expected according to the type of centering applied on multi-block data; t0 centering, in fact, allowed to minimise the differences among batches, highlighting the time

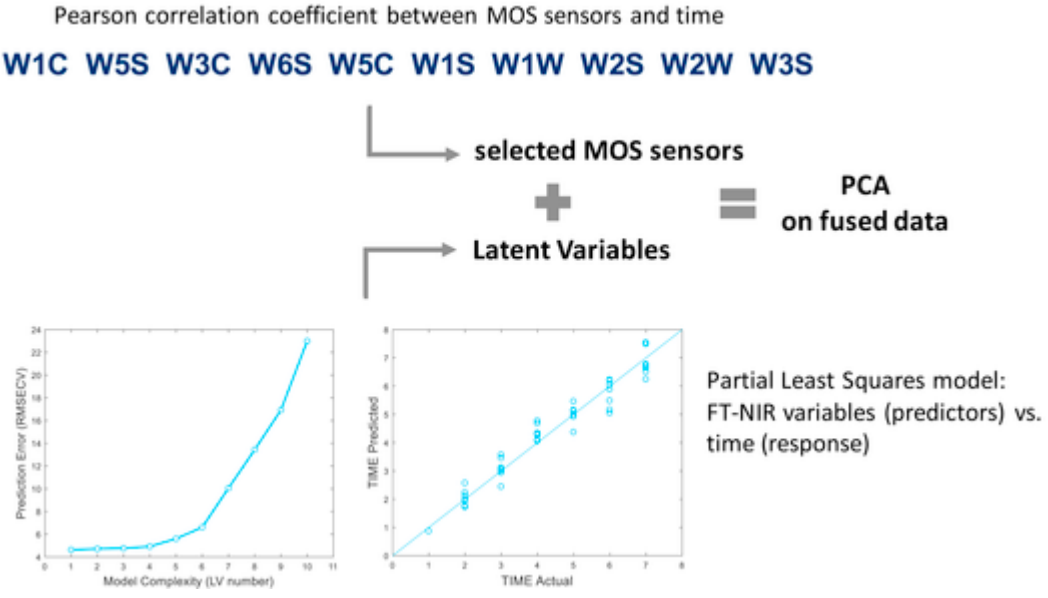

Fig. 3. Scheme of the modified mid-level data fusion approach.

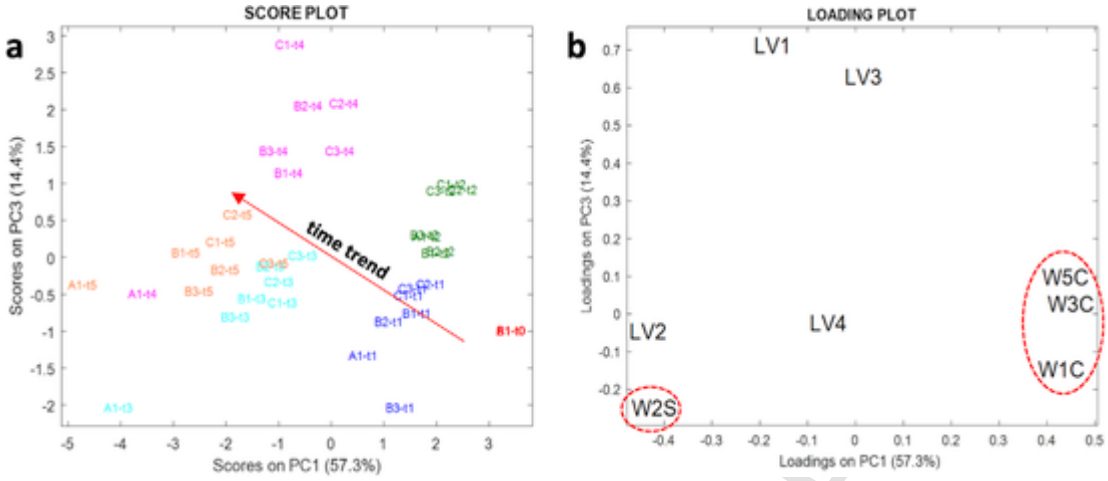

Fig. 4. Outcomes of PCA on fused data: a) score plot PC1 vs. PC3; b) scatter loading plot PC1 vs. PC3.

trend. Variables more accountable for this trend are evidenced in red in Fig. 4b, in which PC loadings are reported; the MOS sensors are the variables that permit the separation of samples according with time. In more detail, sensors belonging to the WC series (W1C, W3C and W5C) are located in the fourth quadrant of the scatter loading plot; the WC series sensors gave higher response for fresh samples (t0, t1 and t2), while rice germ stored for longer time was characterised by the W2S sensor.

In Fig. 5a, scores of the second component (explaining 22.8% of the variance) are reported as scatter plot of PC2 *vs.* PC3; this plot highlights two groups of samples delimited by the ones analysed before storage (t0), which are located close to the axis origin due to t0 centering. No interesting differences are present among samples stored with different SAPs; it means that samples with the same a_w and codified with 1, 2 or 3 are overlapped in the same region of the score plot. Rice germ samples located in the left-bottom corner of the orthogonal space are the ones having higher a_w (samples codified with A), while samples B and C (having a_w equal to 0.45 and 0.36, respectively) are scattered in the opposite portion of the Cartesian space. A joint interpretation with the loading scatter plot (Fig. 5b) shows that this separation is mainly imputable to the FT-NIR block, represented by LV1, LV3 and LV4; these variables are positively related to samples with a lower a_w, while they present a negative correlation with samples with a higher a_w.

Thanks to the reconstruction of loadings of the FT-NIR original variables [32,33], in Fig. 5c it is possible to visualise which NIR bands are mainly involved in defining these LVs. In the line loading plot, two important bands can be highlighted: one around 5700 cm^{-1}, with a high-negative weight in the construction of the new variables, and one around 4000 cm^{-1}, positively related with LVs. Adding this information to the joint interpretation between scores and loadings presented in Fig. 5a and b, it is possible to associate the high absorbance around 5700 cm^{-1} to rice germ samples codified with A, while a high absorbance around 4000 cm^{-1} is linked to samples B and C.

3.2. Correlation between FT-NIR and e-nose sensors

In Fig. 6, the study of correlation between FT-NIR spectra and e-nose sensors is presented. In more detail, the correlation map (Fig. 6a) shows, in a graphical way, the Pearson's correlation coefficients between all the 10 MOS sensors and the whole spectra in the NIR region (4000 - 10,000 cm^{-1}). In the left part of the map, it is possible to visually compare sensors and spectra, while, in the right part, the correlation coefficients between couples of sensors are represented. For an easier understanding of the correlation extent, a colour scale was used. It ranges between blue, codifying negative-strong correlation equal to −1, to red, identifying positive-strong correlation equal to 1, passing throw green for absence of correlation (0); intermediate colours represent weaker correlations. For clarifying the discussion about correlation between families of sensors and NIR bands, the map of a single sensor along the entire spectrum was built. Sensor W2S, as a representative of the WS series (being positively correlated with sensors W1S, W3S, W5S and W6S), and W1C, as a representative of the WC series (being positively correlated with sensors W3C and W5C), are presented in Fig. 6b and c, respectively.

From a comprehensive evaluation of the results presented until now, it is possible to highlight that the W2S sensor is sensitive to compounds characterised by O–H functional groups, which can be considered as markers for sample degradation, in particular as a consequence of lipid oxidation. In more detail, the sensor is positively correlated with two small bands around 6950 cm^{-1} and 10,160 cm^{-1} related with absorption of phenols and alcoholic compounds, respectively.

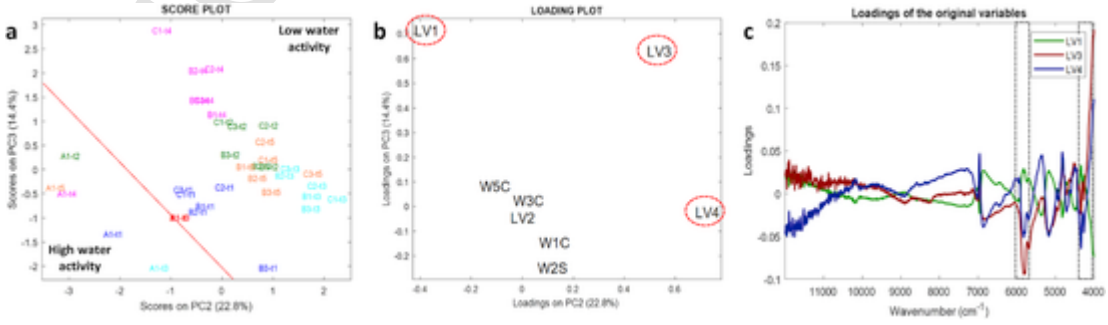

Fig. 5. Outcomes of PCA on fused data: a) score plot PC2 vs. PC3; b) scatter loading plot PC2 vs. PC3; c) FT-NIR loading reconstructed.

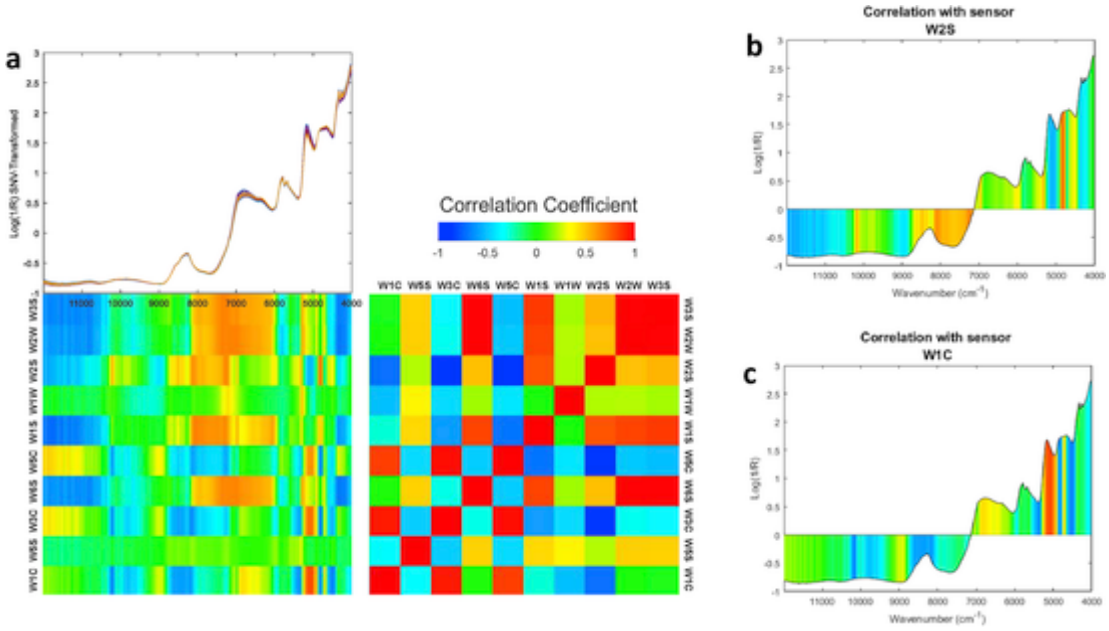

Fig. 6. Outcomes of correlation between FT-NIR and e-nose sensors. a) correlation map between FT-NIR spectra and MOS sensors; b) correlation of sensor W2S with NIR spectrum; c) correlation of sensor W1C with NIR spectra.

NIR bands that are positively correlated with this sensor are those at around 4800–4900 cm^{-1}, which are ascribable to N–H bending of primary amides, typical for peptides coming from protein hydrolysis. Conversely, a negative strong correlation of W2S with the NIR band at 5128 cm^{-1}, imputable to the second overtone of C═O stretching of esters, is encountered; the negative correlation indicates that ester bonds undergo degradation during time [34]. Moreover, W2S, is characterised by high negative values of loadings on PC1 (Fig. 4b), which describe sample trend along time; as a confirmation of the band attribution, it is possible to observe that W2S distinguishes the oldest samples.

For the WC series, an opposite pattern is highlighted, characterised by a negative correlation with the NIR band related to protein degradation, and a positive one with the ester band. This correlation feature describes samples with well-preserved nutritional values. Moreover, all the sensors belonging to the WC series were located in the same quadrant of fresh samples along PC1 (Fig. 4b), corroborating correlation inferences.

Looking at PC2 *vs*. PC3 scores (Fig. 5), jointly with the correlation maps (Fig. 6a), it is possible to notice that the NIR variables mainly responsible for grouping according to a_w are also correlated with families of sensors.

Summarising, samples with a lower a_w present higher intensity of the band around 4000 cm^{-1} (ascribable to phenolic compounds and aromatic derivatives) together with higher responses in the WC sensors (W1C and W3C); for this reason, they can be considered fresh and well preserved. Conversely, samples at higher a_w have a higher absorption in the band at 5700 cm^{-1} (imputable to the first overtone of methylene C–H stretching) and are strongly related with W2S sensor, proving that they underwent degradation along time. In other words, these spectral bands are not directly ascribable to water absorption but to other compounds involved in the chemical pattern of the preservation/degradation state of rice germ samples.

4. Conclusions

This work presents the multiple advantages arising from combining and understanding correlations between non-targeted analytical techniques, with an immediate evidence in the rice germ case study. This approach allowed to evaluate the influence of storage factors on rice germ shelf life, thanks to the combination of two fingerprint methods like spectroscopy and e-nose. The multivariate data processing was the cornerstone for extracting information from a multi-block data array. A data centering was proposed for highlighting the evolution of samples over time, making comparable batches of rice germ stored under different conditions of a_w and SAP. The traditional mid-level data fusion approach was modified to enhance the information related with time; PCA on fused data made possible to understand that a_w, as expected, is the crucial factor for rice germ preservation: the higher a_w, the faster the degradation. Regarding SAPs, no interesting differences were highlighted between air, argon and vacuum for samples having the same a_w. Correlation maps allowed to study the relationship between FT-NIR bands and e-nose non-specific responses, ascribing to the MOS sensors a chemical meaning. In more detail, the W2S sensor, positively correlated with the band around 4800–4900 cm^{-1}, was ascribable to sample decay and, in particular, to protein degradation, while the WC sensors (W1C and W3C), positively related with the absorption band at 5128 cm^{-1}, was related with less deteriorated samples.

References

[1] A. Moongngarm, N. Daomukda, S. Khumpika, Chemical compositions, phytochemicals, and antioxidant capacity of rice bran, rice bran layer, and rice germ, APCBEE Procedia (2012), doi:10.1016/j.apcbee.2012.06.014.
[2] H.R. Sharma, G.S. Chauhan, K. Agrawal, Physico-chemical characteristics of rice bran processed by dry heating and extrusion cooking, Int. J. Food Prop. (2004), doi:10.1081/JFP-200033047.
[3] A. Thanonkaew, S. Wongyai, D.J. McClements, E.A. Decker, Effect of stabilization of rice bran by domestic heating on mechanical extraction yield, quality, and antioxidant properties of cold-pressed rice bran oil (Oryza saltiva L.), LWT - Food Sci. Technol. (Lebensmittel-Wissenschaft -Technol.) (2012), doi:10.1016/j.lwt.2012.03.018.
[4] N. Yilmaz, N.B. Tuncel, H. Kocabiyik, Infrared stabilization of rice bran and its effects on γ-oryzanol content, tocopherols and fatty acid composition, J. Sci. Food Agric. (2014), doi:10.1002/jsfa.6459.
[5] S.S. Patil, A. Kar, D. Mohapatra, Stabilization of rice bran using microwave: process optimization and storage studies, Food Bioprod. Process. (2016), doi:10.1016/j.fbp.2016.05.002.
[6] D. Dhingra, C. Sangeeta, Ohmic heating system for stabilization of rice bran, Agric. Eng. Today 38 (2014) 1–6.
[7] F.T. Orthoefer, J. Eastman, Rice bran and oil, in: E.T. Champagne (Ed.), Rice Chem. Technol., third ed., A.A.C.C. Inc., St.Paul, USA, 2014, pp. 569–593.
[8] J.L. Koontz, Packaging technologies to control lipid oxidation, in: H. Min, J. Charlotte (Eds.), Oxidative Stab. Shelf Life Foods Contain. Oils Fats, Elsevier, 2016, pp. 479–517.
[9] F. Rock, N. Barsan, U. Weimar, F. Röck, N. Barsan, U. Weimar, Electronic nose: current status and future trends, Chem. Rev. (2008), doi:10.1021/cr068121q.

[10] N. Prieto, P. Oliveri, R. Leardi, M. Gay, C. Apetrei, M.L. Rodriguez-Méndez, J.A. De Saja, Application of a GA-PLS strategy for variable reduction of electronic tongue signals, Sens. Actuators B Chem. (2013), doi:10.1016/j.snb.2013.03.114.
[11] O.S. Jolayemi, F. Tokatli, S. Buratti, C. Alamprese, Discriminative capacities of infrared spectroscopy and e-nose on Turkish olive oils, Eur. Food Res. Technol. (2017), doi:10.1007/s00217-017-2909-z.
[12] Y.M. YANG, K.Y. HAN, B.S. NOH, Analysis of lipid oxidation of soybean oil using the portable electronic nose, Food Sci. Biotechnol. 9 (2000) 146–150.
[13] R. Aparicio, S.M. Rocha, I. Delgadillo, M.T. Morales, Detection of rancid defect in virgin olive oil by the electronic nose, J. Agric. Food Chem. (2000), doi:10.1021/jf9814087.
[14] S. Mildner-Szkudlarz, H.H. Jeleń, R. Zawirska-Wojtasiak, The use of electronic and human nose for monitoring rapeseed oil autoxidation, Eur. J. Lipid Sci. Technol. (2008), doi:10.1002/ejlt.200700009.
[15] X. Zheng, Y. Lan, J. Zhu, J. Westbrook, W.C. Hoffmann, R.E. Lacey, Rapid identification of rice samples using an electronic nose, J. Bionics Eng. (2009), doi:10.1016/s1672-6529(08)60122-5.
[16] J. Sung, B.K. Kim, B.S. Kim, Y. Kim, Mass spectrometry-based electric nose system for assessing rice quality during storage at different temperatures, J. Stored Prod. Res. (2014), doi:10.1016/j.jspr.2014.02.009.
[17] B. Zhou, J. Wang, Discrimination of different types damage of rice plants by electronic nose, Biosyst. Eng. (2011), doi:10.1016/j.biosystemseng.2011.03.003.
[18] P. Malaspina, M. Casale, C. Malegori, M. Hooshyari, M. Di Carro, E. Magi, P. Giordani, Combining spectroscopic techniques and chemometrics for the interpretation of lichen biomonitoring of air pollution, Chemosphere 198 (2018), doi:10.1016/j.chemosphere.2018.01.136.
[19] C. De Bleye, P.F. Chavez, J. Mantanus, R. Marini, P. Hubert, E. Rozet, E. Ziemons, Critical review of near-infrared spectroscopic methods validations in pharmaceutical applications, J. Pharm. Biomed. Anal. (2012), doi:10.1016/j.jpba.2012.02.003.
[20] M. Calderisi, A. Ulrici, S. Sinisalo, J. Uotila, R. Seeber, Simulation of an experimental database of infrared spectra of complex gaseous mixtures for detecting specific substances. the case of drug precursors, Sens. Actuators B Chem. (2014), doi:10.1016/j.snb.2013.12.035.
[21] R. Beghi, V. Giovenzana, R. Civelli, C. Malegori, S. Buratti, R. Guidetti, Setting-up of a simplified handheld optical device for decay detection in fresh-cut Valerianella locusta L, J. Food Eng. 127 (2014), doi:10.1016/j.jfoodeng.2013.11.019.
[22] G.D. Batten, A.B. Blakeney, M. Glennie-Holmes, R.J. Henry, A.C. McCaffery, P.E. Bacon, D.P. Heenan, Rapid determination of shoot nitrogen status in rice using near infrared reflectance spectroscopy, J. Sci. Food Agric. 54 (1991) 191–197.
[23] B.G. Osborne, B.J.A. Mertens, M. Thompson, T. Fearn, The authentication of Basmati rice using near infrared spectroscopy, J. Near Infrared Spectrosc. 1 (1993) 77–83.
[24] S. Kawamura, M. Natsuga, K. Takekura, K. Itoh, Development of an automatic rice-quality inspection system, Comput. Electron. Agric., 2003, doi:10.1016/S0168-1699(03)00015-2.
[25] T. Pungseeklao, P. Opanasopit, K. Pramot, Development of a method for quantitative determination of γ-oryzanol using near infrared spectroscopy, Food Appl. Biosci. J. 4 (2016) 107–115.
[26] E. Borràs, J. Ferré, R. Boqué, M. Mestres, L. Aceña, O. Busto, Data fusion methodologies for food and beverage authentication and quality assessment - a review, Anal. Chim. Acta (2015), doi:10.1016/j.aca.2015.04.042.
[27] L. Huang, J. Zhao, Q. Chen, Y. Zhang, Nondestructive measurement of total volatile basic nitrogen (TVB-N) in pork meat by integrating near infrared spectroscopy, computer vision and electronic nose techniques, Food Chem. (2014), doi:10.1016/j.foodchem.2013.06.073.
[28] M. Li, H. Wang, L. Sun, G. Zhao, X. Huang, Application of electronic nose for measuring total volatile basic nitrogen and total viable counts in packaged pork during refrigerated storage, J. Food Sci. (2016), doi:10.1111/1750-3841.13238.
[29] R. Taylor, Interpretation of the correlation coefficient: a basic review, J. Diagn. Med. Sonogr. (1990), doi:10.1177/875647939000600106.
[30] R.J. Barnes, M.S. Dhanoa, S.J. Lister, Standard normal variate transformation and de-trending of near-infrared diffuse reflectance spectra, Appl. Spectrosc. (1989), doi:10.1366/0003702894202201.
[31] F.E. Barton, D.S. Himmelsbach, J.H. Duckworth, M.J. Smith, Two-dimensional vibration spectroscopy: correlation of mid- and near-infrared regions, Appl. Spectrosc. (1992), doi:10.1366/0003702924125375.
[32] V. Pirro, P. Oliveri, C.R. Ferreira, A.F. González-Serrano, Z. Machaty, R.G. Cooks, Lipid characterization of individual porcine oocytes by dual mode DESI-MS and data fusion, Anal. Chim. Acta (2014), doi:10.1016/j.aca.2014.08.001.
[33] R. Simonetti, P. Oliveri, A. Henry, L. Duponchel, S. Lanteri, Has Your Ancient Stamp Been Regummed with Synthetic Glue? A FT-NIR and FT-Raman Study, 2016 Talanta, doi:10.1016/j.talanta.2015.11.059.
[34] J. Workman, L. Weyer, Practical Guide to Interpretive Near-Infrared Spectroscopy, 2007, doi:10.1002/anie.200885575.